Available online at www.sciencedirect.com

ScienceDirect

Energy Procedia 83 (2015) 248 – 257

Energy Procedia

7th International Conference on Sustainability in Energy and Buildings

Development of models for on-line diagnostic and energy assessment analysis of PV power plants: the study case of 1 MW Sicilian PV plant

Cristina Ventura[a]*, Giuseppe Marco Tina[a]

[a]*Dipartimento di Ingegneria Elettrica, Elettronica e Informatica, University of Catania,Catania, 95125, Italy*

Abstract

For photovoltaic (PV) power plants, every kilowatt-hour is important, because only kilowatt-hours that are fed into the grid are remunerated. A plant's operator can only adopt prompt measures to eliminate operational faults when these are immediately signaled. In fact, just reading the feed-in meter each month is not sufficient to promptly recognize faults and to avoid the loss of yields. Many inverters record the most important operational data, automatically evaluate the data and, in case of a fault, send the operator notifications via email or text message. However, it only allows obvious faults to be recorded. On the other hand, continuous, absolute and comparative measurements are necessary to ensure the maximum efficiency and availability. Based on real time and historical data, a technical plant manager should inform the operators of any fault which occurs or even take independent measures to rectify it. In this context, suitable models are developed and applied to a 1 MW power plant where a SCADA, Supervisory Control And Data Acquisition, has been installed and operational data are available on a Web page. In order to evaluate the performance of the PV system, firstly the daily corrected Performance ratio has been evaluated. Then, different approaches to estimate the AC and the DC power of the PV plant have been developed. Basing on the difference between the measured and the estimated power, a statistical approach is proposed; it allows to define suitable thresholds on the AC and DC power in order to individuate a fault when occurs. The experimental results show the effectiveness of the proposed approach.

Peer-review under responsibility of KES International

Keywords: Monitoring; Diagnostic; PV plant; Faults; Statistical analysis

* Ventura Cristina. Tel.: +39-0957382344
E-mail address: cristina.ventura@dieei.unict.it

Peer-review under responsibility of KES International
doi:10.1016/j.egypro.2015.12.179

1. Introduction

Accurate and consistent evaluations of PV system performance are critical for the continuing development of the PV industry. For component manufacturers, performance evaluations are benchmarks of quality for existing products. For research and development teams, they are a key metric for helping to identify future needs. For systems integrators and end customers, they are vital tools for evaluating products and product quality to guide future decision-making.

The development of diagnostic methods for fault detection in the PV systems behavior is particularly important nowadays due to the expansion degree of grid connected PV systems and the need to optimize their reliability and performance. The monitoring and regular performance supervision on the functioning of grid-connected PV systems is necessary to ensure an optimal energy harvesting and reliable power production.

Most diagnostic methods are based on the comparison between monitored data and simulation results of the PV system behavior [1–6]. Monitored climate data, irradiance and temperature are needed for an estimation of the energy produced and the simulation of the PV system behavior in a determinate localization [7, 8]. Furthermore, some works were carried out using artificial intelligent techniques [9–11] and statistical data analysis for supervision of PV systems [12], but these techniques have not been yet optimized for fault detection analysis and clear identification of the kind of fault that occurs in the system.

On the other hand, several researches were also carried out to generate the necessary climate data at the desired location [13–17] or meteorological databases [18, 19] using climate data from satellites observation. These approaches are cost-effective, since no climate sensors are needed on the plant, although they provide low accuracy in estimation of expected energy yield in some specific climatic conditions.

Nowadays, most inverters designed for grid connected PV applications have a wide range of interfaces, in particular sensor inputs and communication interfaces. These sensor inputs can be used to connect irradiance sensors as pyranometers, reference cells and PV module temperature sensors. Therefore, these inverters include monitoring capabilities for irradiance and temperature as well as for maximum power point tracking (MPPT) evolution.

In the fault detection procedure presented in [20], the computational analysis has been reduced avoiding the use of electrical models for simulation of the PV system behavior and the number of monitoring sensors has been minimized. Two indicators of current and voltage are used as benchmarks and the inverter himself can calculate both relationships.

While, in [21] authors present an automatic fault detection method for grid-connected PV plants. The possible faults are recognized using a diagnostic signal. In order to determine the location of the fault, the ratio between P_{DC} and P_{AC} is monitored. The different types of faults that can be identified are: fault in a PV module, fault in a PV string, fault in an inverter, and a general fault that may include partial shading, PV ageing or MPPT error.

Common reference documents for monitoring of PV systems is the standard IEC 61724 [22] and the guidelines of the European Joint Research Centre in Ispra, Italy [23]. In [22, 23] the required accuracies and check procedures for data quality are detailed. Careful considerations should be given to the purpose behind the monitoring before developing a specification. The ethos should be to measure only those variables that are necessary using. Guidelines reported in [1] recommend that parameters which vary directly with irradiance shall be sampled with 1 minute or less interval. Parameters with larger time constants, an arbitrary interval may be specified between 1 min and 10 min. Special consideration for increasing the sampling frequency shall be given to any parameters which may change quickly as a function of system load. However, with the cost of hardware and storage decreasing there is no reason to avoid 1-minute (or sub-minute) data collection. In order to be able to distinguish the performance of the PV system from the variability of the solar resource, monitoring should always include both a measurement of the energy generated and the incoming irradiation. For electricity yield measurements, energy meters or true-rms power meters should be used. The inverter-integrated measurements are usually not sufficiently precise [23]. Nevertheless, they may prove useful for identifying relative changes over time [24]. For more advanced monitoring, the power or current on the junction box level or the string currents should be measured. As part of the European Commission-funded project PERFORMANCE, new PV monitoring guidelines have been recently developed in order to take into account the system performance over its lifetime [25, 26]. Based on these new guidelines, a failure detection routine for comparing the monitored energy yield with the simulated one for a given period was presented in [27, 28]. The additional cost for advanced monitoring depends on the PV plant layout and capacity.

Objective of this study is to propose a new approach for effective detection of faults in grid connected PV systems, which allows to minimize the monitoring system and number of sensors required. The industry factual data of a 1 MW PV Plant (monocrystalline technology) constructed in Agrigento (Italy) is provided. A first study on performance evaluation of the PV plant involves the analysis of the corrected PR methods. Then, the P_{DC} and P_{AC} of the PV plant are estimated with different methods and compared with the measured ones. Basing on the difference between the measured values, a statistical approach is proposed, it allows to define some thresholds that allow to individuate possible faults of the PV system.

Nomenclature

G_{HI}	solar radiation on horizontal plane		
$\bar{x}$	mean value of measured data	P_{DC_STC}	DC power in STC
CPR	daily Corrected Performance Ratio	PR	daily Performance Ratio
CSM	Clear Sky Model	RMSE	Root Mean Square Error
dist	distance between the CSM and G_{POA}	STC	standard test conditions
$E_{PV,m.d}$	monthly average daily energy	T_{PV}	PV module temperature
G_{HI}	solar radiation on horizontal plane	T_{STC}	temperature in STC (T_{STC} = 25°C)
$G_{m,d}$	monthly average daily radiation on the horizontal plane	x_i	measured data
G_{POA}	solar radiation on the plane of array	y_i	estimated data
G_{STC}	solar radiation in STC (G_{STC} = 1000 W/m^2)	α_{PM}	Max power temperature coefficient
M	number of available data	η_{IAM}	power loss due to incident angle
MBE	mean bias error	η_{INV}	inverter theoretical efficiency
nRMSE	normalized Root Mean Square Error	η_{MIS}	efficiency due to mismatch losses
N	number of days when data are available	η_R	power loss due to series resistance
P_{DC}	DC power		

2. Study Case

The data collected to frame this study report is from a 1 MW PV plant situated in Agrigento, Italy. As per official source of data (standard UNI 10349) in Agrigento area, the daily monthly average temperature lies between 10.4÷24.6°C. Moreover, the forecast and measured values of $G_{m,d}$ are shown in Table 1. Under these operating conditions, the system is forecast to produce $E_{PV,m.d.}$ (Table 1). In Table 1, measured values of $E_{PV,m,d}$ are also shown.

Table 1. Forecasted and measured values of G_m and $E_{PV,m}$ in Agrigento (latitude 37° 31' N, longitude 13° 58' E, altitude 230m, Italy).

Month	Jan	Feb	Mar	Apr	May	Jun	Jul	Aug	Sep	Oct	Nov	Dec
$G_{m,d}$ (kWh/m^2)	2.44	3.47	4.69	6.17	7.47	8.19	8.22	7.5	5.81	4.06	2.81	2.28
$G_{m,d}$ (kWh/m^2) Meas.	**1.48**	**0.98**	**1.21**									**2.72**
$E_{PV,d}$ (kWh)	2226	2992	3804	4762	5555	5985	6051	5719	4642	6441	2532	2129
$E_{PV,m}$ (kWh) Meas.	**1144**	**816**	**910**									**2230**

The PV plant is equipped with 5404 monocrystalline Si modules each of 180 – 185 Watts and 3 inverters. The main characteristic of the PV plant, of the PV modules and of the inverters are reported in Table 2.

Table 2. Main characteristic of the PV plant.

PV plant	
Annual total energy (kWh)	1 518 128.96
P_{DC_STC} **(kW)**	• Total 987.08 • Inverter 1: 348.13 • Inverter 2: 308.48 • Inverter 3: 330.47
Num. PV modules	5404
Num. inverters	3
Num. of strings per inverter	119 – 126 - 140

PV module	
Tilt/Azimuth (°)	12/18
Type	Monocrystalline
Model	UPSOLAR - M180M
P_p **(W)**	180 - 185
V_{mppt} **(V)**	35.80
I_{mppt} **(A)**	5.03
V_{oc} **(V)**	44.60
I_{sc} **(A)**	5.38
μ_{Voc} **(%/°C)**	-0.32
μ_{Isc} **(%/°C)**	0.05

Inverter	
Model	ELETTRONICA SANTERNO - SUNWAY TG 385 800 V
$V_{mppt,min}$ **(V)**	430
$V_{mppt,max}$ **(V)**	760
$I_{max,DC}$ **(A)**	657.6
$P_{max,DC}$ **(kW)**	362.4
P_{AC} **(kW)**	294.6
$P_{max,DC}$ **(kW)**	362.4

The data are recorded by a SCADA system through the Met station installed in the plant premises and trivector (TVM) meters. The stored data are: G_{HI}, G_{POA}, T_{PV}, ambient temperature, DC current and voltage of each of the 3 inverters; and AC current and voltage of each of the 3 inverters. To measure T_{PV}, two 4 lines Pt100 (class B) temperature sensors (-20 + 120 °C) have been used. Then, a temperature transmitter for Pt100 in with 4 - 20 mA analogue output has been used to acquire temperature data. The temperature values are the result of the average value of the temperature measured on two strings. While the ambient temperature has been measured using a mineral insulated platinum thermoresistance with metal sheath. Two LP PYRA 02 pyranometers have been used to measure G_{HI} and G_{POA}. Then, a Thytronic NV10P interface protection control unit has been used for monitoring voltage and frequency relay. Moreover, a Seneca T201DC, that is an isolated, contact-less loop powered direct current transducer (4 to 20 mA), has been used to measure the current. Solar radiation, DC and AC voltage and DC and AC current are acquired every minute, while temperature values are acquired with a 5 minutes timestamp since they present a slower dynamic. Then, an interpolation of the values is done in order to have a value of temperature each minute correspondent to the other parameters.

3. Monitoring and diagnostic methods

3.1. Corrected performance ratio

Various indices can be used for monitoring and diagnostic purposes, the most important and most authentic metric to analyze the performance of a PV plant is the *PR*. It is defined in IEC 61724 and is a metric to measure how effectively the plant converts sunlight collected by the PV modules into AC energy despite of many derating factors. Conventionally *PR* is calculated as Eq. (1), however this equation does not incorporate any factors except irradiance. Yet it is very important to consider the effect of temperature and module efficiency along with PV area to calculate the *CPR*. Along with solar insolation, in fact, temperature also plays a big role in affecting the efficiency of a PV plant. *PR* is often corrected to a common temperature of 25°C (standard test conditions) as mentioned in Eq. (2).

$$PR_d = \frac{\sum_{i=1}^{M} P_{ACi}}{\sum_{i=1}^{M} P_{DC\_STC} \cdot \left(\frac{G_{POAi}}{G_{STC}}\right)} \quad (1)$$

$$CPR_d = \frac{\sum_{i=1}^{M} P_{ACi}}{\sum_{i=1}^{M} P_{DC\_STC} \cdot \left(\frac{G_{POAi}}{G_{STC}}\right) \cdot \left(1 + \alpha_{PM} \cdot (T_{PV} - T_{STC})\right)} \quad (2)$$

where α_{PM} is usually provided by module manufacturer (α_{PM} = 0.45 %/°C).

3.2. AC power estimation

A simple method for the inefficiency estimation is based on the comparison between the measured and the estimated P_{AC} in operating conditions.

There are several correlations in the literature to estimate the PV electrical power as a function of cell/module operating temperature and basic environmental variables [29].

3.2.1. Physical approach

The first solution here proposed is based on a physical modelization of the power. In the operating conditions, it depends on the power measured at STC (P_{DC_SCT}) and can be estimated through Eq. 3. Eq. (3) takes into account only the power losses due to temperature; therefore using it, the power is always overestimated. Consequently, other causes of power losses should be modelized and considered to better estimate P_{AC}. First of all, the power losses caused by incident angle related to direct and diffuse irradiance have been taken into account (η_{IAM}) [30]. Then, also mismatch losses, due to variations in PV module current-voltage curves have been added. There are different causes that can provoke module mismatch, which usually are between 1-9% [14]. For the sake of simplicity, in this paper η_{MIS} has been taken into account as a constant loss during simulation, in particular η_{MIS} has been evaluated through the *PVSyst* software considering the design of the PV plant here studied [31] (η_{MIS}=98%).

$$P_{DC-phy\_1} = P_{DC\_STC} \cdot \frac{G_{POA}}{G_{STC}} \cdot \left(1 - \alpha_{PM} \cdot (T_{PV} - T_{STC})\right) \quad (3)$$

$$P_{DC-phy\_2} = \eta_{IAM} \cdot \eta_{Mis} \cdot P_{DC-phy\_1} \quad (4)$$

Moreover, when power output is generated by solar irradiation on a PV module, Joule heating loss occurs by an electric current to flow through a circuit [32]. Consequently, η_R can be determined by current flowing in a PV

module (I) and series resistance (R) [33]. Therefore, to calculate η_R, R should be calculated. In this case, if no other losses are taken into account, R can be calculated by least square fits.

$$\eta_R = \frac{P_{DC\_phy\_2}}{P_{DC\_phy} + R \cdot I^2} \quad (5) \qquad P_{DC-phy} = P_{DC-phy\_2} - R \cdot I^2 \quad (6)$$

Finally, to estimate P_{AC}, η_{INV} should be considered, which is indicated, with respect to the percentage of the maximum output power, in the datasheet of the inverter:

$$P_{AC-phy} = \eta_{INV} \cdot P_{DC-phy} \quad (7)$$

3.2.2. Fitting approaches

In order to predict power it is also possible to use polynomial regression models [29]. An example is reported in [34]; the model consists of a polynomial fit to operational data where the power produced by the system is a function of the incident global irradiance in the plane of the array and the PV array module temperature, it is described by the following equation [34]:

$$P_{AC-fit1} = A + B \cdot T_{PV} \cdot G_{POA} + C \cdot G_{POA} + D \cdot G_{POA}^2 \quad (8)$$

where A, B, C and D are polynomial constants determined by least square fits.

Another example is proposed in [35]:

$$P_{AC-fit2} = D_1 \cdot G_{POA} + D_2 \cdot T_{PV} + D_3 \cdot [\ln G_{POA}]^m + D_3 \cdot T_{PV} \cdot [\ln G_{POA}]^m \quad (9)$$

also in this case $D_{1\text{-}4}$ and m are polynomial constants determined by least square fits.

These simulation procedures require first the calibration of the model to the system under study in order to obtain the polynomial constants that best represent the behaviour of the system. Once the model is well adjusted, the same constants are used along with new temperature and irradiance inputs to predict the power generated by the system.

3.3. Parameters estimation

In order to estimate the parameters involved in the physical approach (R) and in the fitting approaches (A, B, C, D, D_1, D_2, D_3, D_4 and m), only some of the whole set of the available data (from 1st December 2014 to 31st March 2015) should be used. To choose this reduced set of data in such a way to optimize the parameters estimation, it is convenient to choose data relative to clear sky days. To this aim, the algorithm whose block diagram is shown in Fig. 1, has been used. It allows to choose the set of data to be used to estimate the parameters in an automatic way. Firstly, the profile of the solar radiation of a clear sky day using the CSM proposed in [36] on an inclined surface, has been generated for each day of available data. The distance, *dist*, is calculated as the sum of their difference minute per minute. If *dist* is greater than a threshold, that has been heuristically set to 240 kW/m^2, the analyzed day is considered as a clear day and therefore G_{POA}, T_{PV} and P_{AC} profiles of that day are used to estimate the parameters.

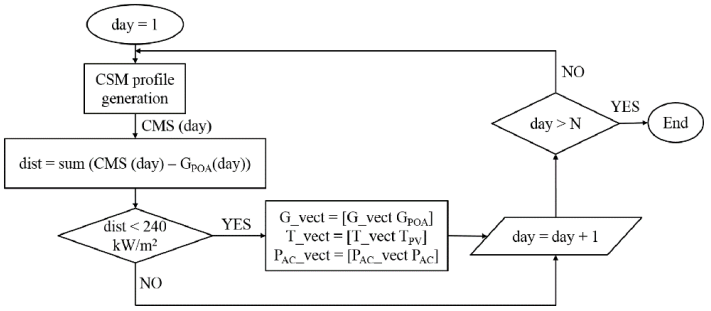

Fig. 1. Block diagram of the algorithm used to choose the set of data to estimate the parameters of the physical and the fitting approaches.

For assessing the quality of the identified parameters and the estimated P_{AC} though the three approaches here proposed, different statistical parameters have been used: *MBE, RMSE* and *nRMSE*, which is a non-dimensional form of the error, have been calculated.

$$MBE = \sum_{i=1}^{M} (y_i - x_i)^2 \Big/ M \cdot \bar{x} \quad (10) \qquad RMSE = \sqrt{\frac{1}{M} \cdot \sum_{i=1}^{M} (y_i - x_i)^2} \quad (11) \qquad nRMSE = \sqrt{\sum_{i=1}^{M} (y_i - x_i)^2} \Big/ \sqrt{\sum_{i=1}^{M} (x_i)^2} \quad (12)$$

4. Fault identification

After having estimated P_{AC} with the three approaches here proposed, using the statistical parameters of Eq. 10 - 12, it is possible to establish which is the method that allows to better approximate P_{AC}. Then, it is possible to calculate the difference between the measured and the estimated P_{AC}. A statistical analysis of the values of this difference can allow to identify possible faults on the system.

The adopted procedure is described below. First of all, minute per minute of each available day, the difference between the estimated and the measured P_{AC} of each inverter is calculated:

$$diff_{P_{AC}} - INVi(day, \min) = P_{AC-estimated}(\min) - P_{AC-meas}(day, \min) \qquad i = 1, 2, 3 \qquad (13)$$

where $P_{AC\text{-}estimated}$ is the P_{AC} estimated with one of the three methods here proposed. Then the probability distribution of $diff_{PAC}\_INV\_i$ is obtained per each inverter.

In order to individuate a possible situation of fault, the interval of the $diff_{PAC}$-*INVi* values in which lies a certain percentage of probability should be identified. To this aim, firstly a Kolmogorov-Smirnov test to compare the $diff_{PAC}$-*INVi* probability distribution with other known probability distributions (such as the normal distribution, gamma distribution, etc.) has been applied, but no likenesses have been found. Therefore, to find the interval of $diff_{PAC}$-*INVi* values, all the possible intervals in which the given percentage of the total area lies are identified. Then, the interval whose mean value is the most near to the mean value of the $diff_{PAC}$-*INVi* probability distribution is found. The extremes of this interval are then used to identify possible faults in the PV system. In particular, if the value of $diff_{PAC}$-*INVi* is out of the interval for more than 5 minutes, an alarm occurs. In order to verify if the fault is in the DC side or in the AC side, when an alarm occurs, the same procedure is applied to the difference between the estimated and the measured P_{DC}. The interval for the $diff_{PDC}$-*INVi* values is found, if $diff_{PDC}$-*INVi* is out of it, it means that the fault concerns the DC side, otherwise the fault affects the inverter.

5. Experimental Results

5.1. Data analysis

In order to estimate P_{AC} produced by each inverter, the physical (Eq. 7) and the fitting (Eq. 8 and Eq. 9) approaches proposed in Sec. 4 have been considered. Fig. 2.a shows an example of the obtained results. As it is possible to note, the three methods allow to estimate the power with a good accuracy except for the first hours after sunrise; this is due to shading problems on the pyranometer used to measure G_{POA}. To solve this problem that can lead to individuate false fault problems, in the case the estimated efficiency with the physical method, $P_{DC\text{-}phy\_2}$ (which represents the maximum value that P_{DC} can assume in any specific conditions), is lower that the measured P_{DC}, G_{POA} is calculated from the measured P_{DC} value. In particular, by plotting the measured P_{DC} of each inverter vs G_{POA}, the new value of the solar radiation is calculated using the equation resulting by the interpolating line data, shown in Fig. 2.b.

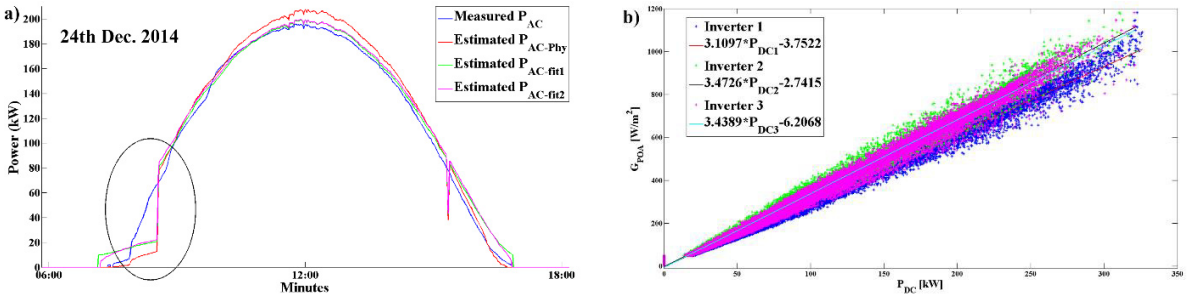

Fig. 2. Shading problems; (a) Comparison between measured and estimated P_{AC} for inverter 1, which shows the shading problems of the solar radiation sensor; (b) P_{DC} vs G_{POA} and interpolating equations for each of the 3 inverters.

Considering the profile of the G_{POA} after having eliminated the shading problems and using the set of the data chosen using the algorithm shown in Fig. 1, the parameters of the different approaches here used to estimate the P_{AC}

of the three inverters have been estimated by least square fits.

Moreover, in the physical approach, to estimate the P_{AC}, Eq. 7 is used, where η_{INV} represents the theoretical inverter efficiency. Nevertheless, the inverter efficiency is not always equal to that one indicated in the datasheet.

Therefore, P_{AC} of each of the three inverters has been estimated using the different approaches here proposed. Table 3 summarizes the obtained results in terms of *MBE*, *RMSE* and *nRMSE*.

Table 3. Values of *MBE*, *RMSE* and *nRMSE* for the three inverters. Data are available from 1st December 2014 to 31st March 2015.

	Inverter 1			Inverter 2			Inverter 3		
	MBE (%)	**RMSE**	**nRMSE (%)**	**MBE (%)**	**RMSE**	**nRMSE (%)**	**MBE (%)**	**RMSE**	**nRMSE (%)**
$\mathbf{P_{AC\_phy}}$	3.96	11.71	14.75	1.10	9.68	13.40	4.69	10.79	14.74
$\mathbf{P_{AC\_fit1}}$	1.33	15.48	19.48	2.42	13.00	19.36	2.62	14.22	19.43
$\mathbf{P_{AC\_fit2}}$	0.35	15.51	19.52	1.56	14.02	19.40	2.08	14.24	19.47

5.2. Fault identification

Firstly, the *PR* and the *CPR* have been calculated (Fig. 3). Then, the statistical analysis has been applied to the available data to recognize possible faults in one of the three inverters.

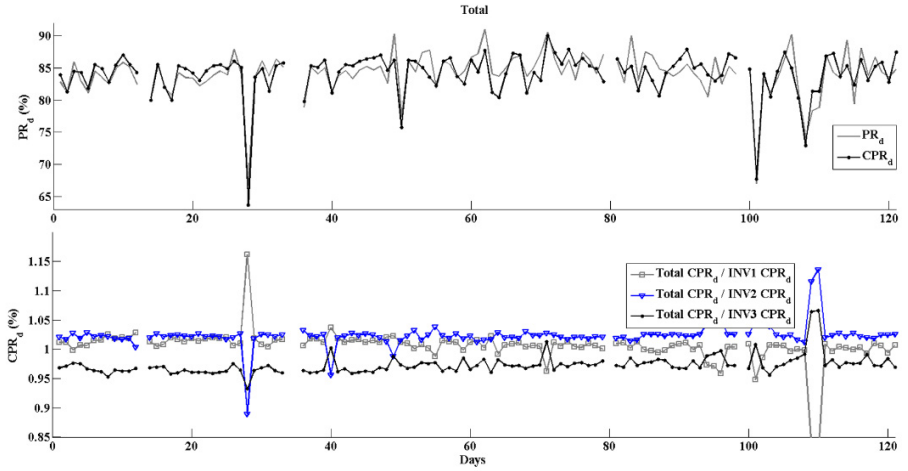

Fig. 3. PR and CPR of the total PV plant and the *CPR* of each inverter with respect to the total *CPR*.

Fig. 4 shows the probability distribution of $diff_{PAC}$-*INV1*, using the physical approach (Eq. 7) to estimate P_{AC}, where the extremes of the interval in which the 90% of probabilities lie, their mean value and the mean value of the distribution are also indicated. The probability distribution of $diff_{PAC}$*_INV_2* and $diff_{PAC}$*_INV_3* are similar to that one shown in Fig. 5.a. The shape of these probability distributions have two peaks, therefore there are two values of $diff_{PAC}$-*INVi* that have high probability of happening. Indeed, the probability distribution should be a unique peak corresponding to the null value of $diff_{PAC}$-*INVi*, as it happens in the probability distribution of $diff_{PDC}$-*INVi* (Fig. 5.b), therefore these results could indicate problems to the inverter efficiency. The extremes values have been used as threshold to identify possible faults in the PV system.

As an example, in Fig. 5.a the days in which the $diff_{PAC}$-*INV1* values are greater than P_{AC}-thH-INV1 for more than 5 minutes are shown. In this case the alarm state is set to 1, 0 otherwise. When an alarm occurs, the $diff_{PDC}$-*INV1* is analyzed. If $diff_{PDC}$-*INV1* values are greater than P_{DC}-*thH-INV1*, it means that the fault concerns the DC side of the PV system, otherwise it is due to a problem in the inverter 1. While in Fig. 5.b the days in which the $diff_{PAC}$-*INV1* values are lower than P_{AC}-thL-INV1 for more than 5 minutes, are shown. Also in this case the alarm state is set to 1, 0 otherwise. The same procedure is applied to inverter 2 and 3.

Fig. 5.a shows how the low threshold is almost always due to a problem in the DC side, since the cause could be attributed to sensors problems. While Fig. 5.b shows how it is possible to discern if the fault is in the AC side of the analysed inverter, in this case only the efficiency state of P_{AC} will be equal to 1, while if simultaneously also the efficiency state of P_{DC} is equal to 1, it means that the fault is in the DC side.

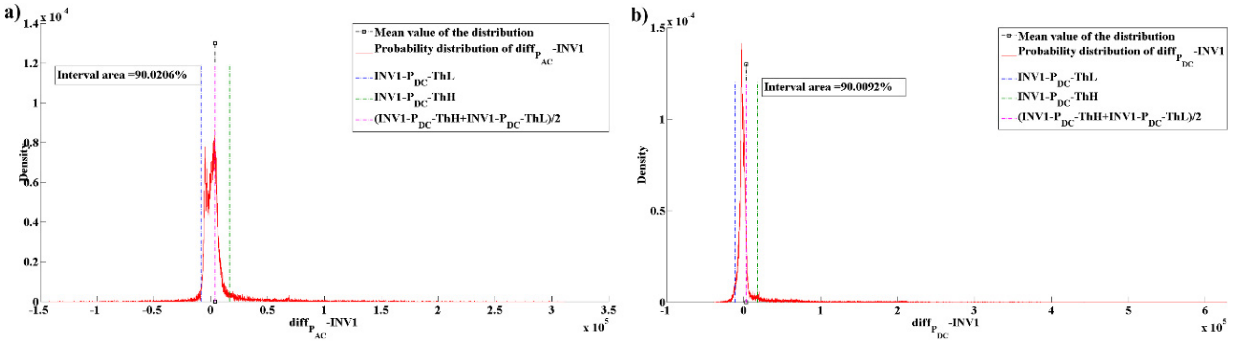

Fig. 4. Probability distribution of: a) *diff$_{PAC}$_INV_1;* b) *diff$_{PDC}$_INV_1*. The green and black dashed lines represent the interval in which 90.02% of the values lie, the magenta dashed line represent their mean value, while the black dashed line represents the mean value of the distribution.

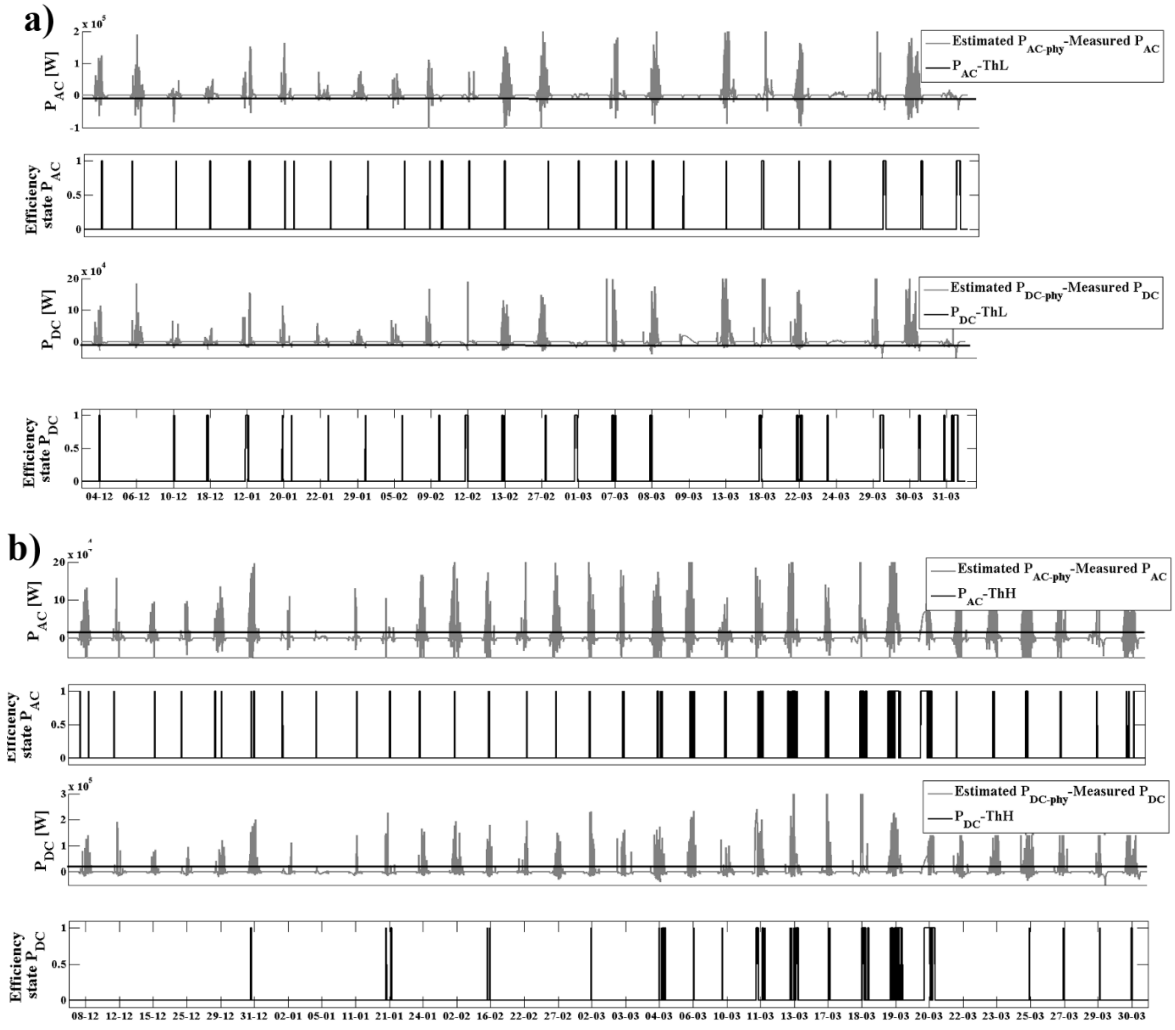

Fig. 5. Example of the alarm occurred in the inverter 1; (a) because the low threshold of *diff$_{PAC}$-INV1* and/or *diff$_{PDC}$-INV1* have been exceeded; (b) because the high threshold of *diff$_{PAC}$-INV1* and/or *diff$_{PDC}$-INV1* has been exceeded. The efficiency state is equal to one in case of inefficiency of the PV system.

6. Conclusions

The goal of this study is to develop models and methodologies that allow monitoring and diagnostics of a PV system in order to increase its manufacturability, efficiency and reliability.

A simple monitoring system that measures in real time the operating parameters of the PV system can allow the detection of discontinuity operation or malfunctioning, but does not provide sufficient information to define whether the performance of the PV system are the highest for the specific environmental conditions or a fault occurs. To this aim, the first parameter that has been here proposed is the daily corrected performance ratio that, taking into account the effect of temperature, gives an indication of the performance of the PV system of any specific day. If quantities provided by a monitoring system of a PV system are used to identify a malfunctioning, they must be compared to a reference value. To this purpose, a physical approach and two fitting approaches have been proposed to estimate P_{DC} and P_{AC} of each inverter in any specific condition. Basing on the difference between the measured and the estimated P_{DC} and P_{AC}, a statistical approach has been proposed for monitoring and diagnostic aims. In particular, it allows to set opportune thresholds that can be used to individuate and locate a fault in the PV system.

A 1 MW PV plant situated in Agrigento, Italy, has been taken as test-bed. It is equipped with 5404 monocrystalline Si modules each of 180 – 185 Watts and 3 inverters. A solar radiation sensor and a temperature sensor have been installed. A SCADA system allows to store environmental variables, the irradiance on the plane of array, the module surface temperature, DC and AC current and voltage of each of the 3 inverters. Basing on this information, using the statistical approach here proposed, situation in which there is a fault on one of the inverter for more than 5 minutes can be detected, it is also possible to distinguish if the fault concerns the DC or the AC side or if there are measurement problems. However, it only allows to detect faults at inverter level.

On the other hand, to obtain a good compromise between cost and performance, a semi-distributed monitoring and supervision system, in which the monitoring is carried out at the level of the string or group of strings, should be considered. Actually, the available information on the PV plant here analyzed does not allow to exactly locate the faulty strings. Therefore, next step is to install a current sensor on each string; analyzing the current of each specific string, in fact, not only will allow to precisely locate the fault, but will also give more information to distinguish among different causes of fault.

Acknowledgements

This work is developed under the ICARO project funded by the POR FESR Sicilia 2007-2013 program (Linea di intervento 4.1.1.1).

References

[1] Yagi Y, Kishi H, Hagihara R, Tanaka T, Kozuma S, Ishida T, et al. Diagnostic technology and an expert system for photovoltaic systems using the learning method. Sol Energy Mater Sol Cells 2003; 75:655–63.

[2] Chao KH, Hob SH, Wang MH. Modeling and fault diagnosis of a photovoltaic system. Electric Power Syst Res 2008; 78:97–105.

[3] Chouder A, Silvestre S. Automatic supervision and fault detection of PV systems based on power losses analysis. Energy Convers Manage 2010; 51: 1929–37.

[4] Gokmen N, Karatepe E, Celik B, Silvestre S. Simple diagnostic approach for determining of faulted PV modules in string based PV arrays. Sol Energy 2012; 86: 3364–77.

[5] Silvestre S, Chouder A, Karatepe E. Automatic fault detection in grid connected PV systems. Sol Energy 2013; 94: 119–27.

[6] Trillo-Montero D, Santiago I, Luna-Rodriguez JJ, Real-Calvo R. Development of a software application to evaluate the performance and energy losses of grid-connected photovoltaic systems. Energy Convers Manage 2014; 81:144–59.

[7] Forero N, Hernández J, Gordillo G. Development of a monitoring system for a PV solar plant. Energy Convers Manage 2006; 47: 15–6.

[8] Chouder A, Silvestre S, Taghezouit B, Karatepe E. Monitoring, modeling and simulation of PV systems using LabVIEW. Sol Energy 2013; 91: 337–49.

[9] Ducange P, Fazzolari M, Lazzerini B, Marcelloni F. An Intelligent system for detecting faults in photovoltaic fields. In: Proc. of the 11th international conference on intelligent systems design and applications (ISDA), 2011, p. 1341–6.

[10] Mellit A, Kalogirou SA. ANFIS-based modelling for photovoltaic power supply system: a case study. Renew Energy 2011; 36: 250–8.

[11] Syafaruddin, Karatepe E, Hiyama T. Controlling of artificial neural network for fault diagnosis of photovoltaic array. In: IEEE 16th international conference on intelligent system application to power systems, 2011, p. 1–6.

[12] Vergura S, Acciani G, Amoruso V, Patrono GE, Vacca F. Descriptive and inferential statistics for supervising and monitoring the operation of PV plants. IEEE Trans Ind Electronics 2009; 56: 4456–63.
[13] Muselli M, Notton G, Canaletti JL, Louche A. Utilization of meteosat satellite-derived radiation data for integration of autonomous photovoltaic solar energy systems in remote areas. Energy Convers Manage 1998; 39:119.
[14] Stettler S, Toggweiler P, Remund J. Spyce: satellite photovoltaic yield control and evaluation. In: Proc. of the 21st European photovoltaic solar energy conference, 2006, p. 2613–2616.
[15] Drews A, de Keizer AC, Beyer HG, Lorenz E, Betcke J, Van Sark WGJHM, et al. Monitoring and remote failure detection of grid-connected PV systems based on satellite observations. Sol Energy 2007; 81: 548–64.
[16] Fernández-Pacheco DG, Molina-Martínez JM, Ruiz-Canales A, Jiménez M. A new mobile application for maintenance tasks in photovoltaic installations by using GPS data. Energy Convers Manage 2012; 57: 79–85.
[17] Tadj Mohammed, Benmouiza Khalil, Cheknane Ali, Silvestre Santiago. Improving the performance of PV systems by faults detection using GISTEL approach. Energy Conversion and Management 2014; 80: 298–304.
[18] Quesada B, Sánchez C, Cañada J, Royo R, Payá J. Experimental results and simulation with TRNSYS of a 7.2 kWp grid-connected photovoltaic system. Appl Energy 2011; 88: 1772–83.
[19] Hernandez J, Gordillo G, Vallejo W. Predicting the behavior of a grid-connected photovoltaic system from measurements of solar radiation and ambient temperature. Appl Energy 2013; 104: 527–37.
[20] Santiago Silvestre, Mário Aires da Silva, Aissa Chouder, Daniel Guasch, Engin Karatepe, New procedure for fault detection in grid connected PV systems based on the evaluation of current and voltage indicators, Energy Conversion and Management 2014; 86: 241-249.
[21] Chine W, Mellit A, Pavan AM, Kalogirou SA. Fault detection method for grid-connected photovoltaic plants. Renew Energy 2014; 66: 99–110.
[22] Blaesser G and Munro D. Guidelines for the Assessment of Photovoltaic Plants Document A Photovoltaic System Monitoring. Commission of the European Communities, Joint Research Centre, Ispra, Italy, EUR 16338 EN, Issue 4.2, 1995.
[23] Report IEA PVPS T3-03: 2014 “Analytical Monitoring of Grid-connected Photovoltaic Systems: Good Practices for Monitoring and Performance Analysis”, March 2014.
[24] Woyte A, Richter M, Moser D, Mau S, Reich N, Jahn U. Monitoring of Photovoltaic Systems: User Stories and Interpretation Guidelines. 28th European Photovoltaic Solar Energy Conference and Exhibition 2013 Paris, France.
[25] Pearsall N M and Atanasiu B. Assessment of PV System Monitoring Requirements by Consideration of Failure Mode Probability,” in 24th EUPVSEC, Hamburg, Germany, 2009, p. 3896 – 3903.
[26] Stettler S, Toggweiler P, E. Wiemken, W. Heydenreich, A. C. de Keizer, W. van Sark, S. Feige, M. Schneider, G. Heilscher, and E. Lorenz, “Failure detection routine for grid - connected PV systems as part of the PVSAT-2 project,” in 20th EUPVSEC, Barcelona, Spain, 2005, p. 2490–2493.
[27] Drews A, De Keizer A C, Beyer H G, Lorenz E, Betcke J, Van Sark W, Heydenreich W, Wiemken E, Stettler S and Toggweiler P. Monitoring and remote failure detection of grid-connected PV systems based on satellite observations. Solar Energy 2007; 81 (4): 548–564.
[28] Oozeki T, Izawa T, Otani K and Kurokawa K. An evaluation method of PV systems. Solar Energy Materials and Solar Cells 2003; 75 (3): 687–695.
[29] Skoplaki E and Palyvos J A. On the temperature dependence of photovoltaic module electrical performance: A review of efficiency/power correlations. Solar Energy 2009, 83 (5): 614-624.
[30] D. Rojas, J. Beermann, S.A. Kleinand D.T. Reindl. Thermal performance testing of flat-plate collectors. Solar Energy 2008; 82 (8): 746–757.
[31] PVSYST SA, "PVSYST", Download PVSYST, [Online] http://www.pvsyst.com/.
[32] Norton B, Eames P C, Mallick T K, Huang M J, McCormack S J, Mondol J D and Yohanis Y G. Enhancing the performance of building integrated photovoltaics. Solar Energy 2011; 85 (8): 1629-1664.
[33] Okada N, Yamanaka S, Kawamura H, Ohno H and Kawamura H. Diagnostic method of performance of a PV module with estimated power output in considering four loss factors. Photovoltaic Specialists Conference, 2005. Conference Record of the Thirty-first IEEE, p. 1643-1646, 3-7 Jan. 2005.
[34] Mayer D, Wald L, Poissant Y, Pelland S. Performance prediction of grid-connected photovoltaic systems using remote sensing. Report IEA-PVPS T2-07.
[35] Rosell J L, Ibànez M. Modelling power output in photovoltaic modules for outdoor operating conditions. Energy Conversion and Management 2006; 47: 2424–2430.
[36] Masters GM, Renewable and Efficient Electric Power Systems, 2nd Edition, August 2013.